

Appreciating Current Trends in LPDAs

L. B. Cebik, W4RNL

Modern log-periodic dipole arrays (LPDAs) serve a wide variety of applications throughout the RF spectrum. Wherever the user requires a wide operating frequency range with relatively equal performance across the passband, LPDAs find service. LPDAs belong to a class of “frequency-independent” antenna designs, wherein the geometry of the antenna is the crucial factor in setting the performance level and the frequency span covered. The apex angle, α , together with length and spacing factors τ and σ , provide much of what one needs to design an LPDA. In fact, the process is amenable to computer-based design. The most-used program may be Roger Cox’s LPCAD (3.1), a reliable DOS program.

Despite the precision of the geometric aspects of LPDA design, the electronic portions of most equation sets are fraught with approximations that are crucial to tailored final designs. Off the rack, basic computer-based (or even hand-calculated) designs will work after a fashion. However, as I noted in the open chapter of *LPDA Notes*, Volume 1, the equations are simply a starting point. Refinement requires analysis of the design and adjustment to bring the array into full compliance with any tight specifications set out for the LPDA. The normal vehicle for performance these pre-prototype refinements is antenna modeling software, such as NEC or MININEC.

Despite the title of these notes, our goal is not to survey contemporary LPDA designs. The expression “current trends” refers to the progression of current magnitude along the series of elements forming an LPDA. Those currents have much to tell us about the anticipated performance of the antenna at all frequencies. After some preliminary reflections on the electronic portions of the typical set of design equations, we shall explore just what those current progressions tell us about potential performance and what adjustments may be wise to make to the initial design.

Design Equation Limitations

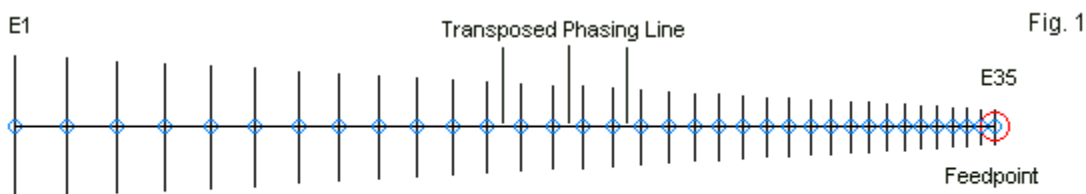
The geometry of an LPDA is well described in many sources, dating back to the earliest papers in the late 1950s and early 1960s. One often-used progression appears in Chapter 1 of *LPDA Notes* and in Chapter 10 of *The ARRL Antenna Book*. (See endnote 1.) I shall not repeat the entire sequence here. The terms α , τ , and σ are inter-related so that we may create a design using only 2 of them. Most often, design equations use τ and σ . Values of τ may run from about 0.8 to 0.98, with the upper end of the range being most common in advanced LPDA designs. (To reduce the number of elements per unit length, amateur upper-HF designs often use lower values of τ , sometimes down to about 0.85.) For every value of τ , there is an optimum value of σ , defined by the following equation.

$$\sigma_{opt} = 0.243\tau - 0.051$$

All of the sample LPDAs that we shall encounter use a τ of 0.96, with its optimum σ of 0.18. In fact, we shall employ only two basic models (with variations): a 5-30-MHz 56-element array and a 14-30-MHz upper-HF antenna. Because of its more compact model size and its ability to illustrate virtually all of the points that we wish to consider, the latter design will be the primary sample.

Fig. 1 outlines the structure of the antenna and its NEC-4 model. The horizontal line indicates the transposed phase line that interconnects the elements. The feedpoint occurs at

the junction of this line and the shortest element in the group. The outline sketch shows 35 elements, although we shall also consider briefly a shorter 31-element version of the same antenna.



General Outline of a 14-30 MHz Standard LPDA with Tau = 0.96, Sigma = 0.18

The sketch lists the elements from the longest to the shortest. For the array at hand, **Table 1** provides the LPDA dimensions with respect to element length and spacing. Spacing counts from the rearmost element forward. The table also lists element half-lengths for anyone who wishes to recreate the model. The dividing line below element 31 establishes that except for the added elements, the shorter and longer arrays are identical.

14-30 MHz Tau .96, Sigma .18 LPDAs								Table 1
Dimensions and Spacing in Inches								
Element	Space	Length	1/2 Len	Element	Space	Length	1/2 Len	Limit
1	0.00	430.14	215.07	19	2014.63	206.30	103.15	
2	154.85	412.94	206.47	20	2088.90	198.05	99.02	
3	303.51	396.42	198.21	21	2160.20	190.13	95.06	
4	446.23	380.56	190.28	22	2228.64	182.52	91.26	
5	583.23	365.34	182.67	23	2294.35	175.22	87.61	
6	714.76	350.74	175.37	24	2357.43	168.21	84.11	
7	841.02	336.70	168.35	25	2417.99	161.48	80.74	
8	962.23	323.24	161.62	26	2476.12	155.02	77.51	
9	1078.59	310.30	155.15	27	2531.93	148.82	74.41	
10	1190.31	297.90	148.95	28	2585.50	142.87	71.44	
11	1297.55	285.98	142.99	29	2636.94	137.16	68.58	
12	1400.50	274.54	137.27	30	2686.31	131.67	65.84	
13	1499.33	263.56	131.78	31	<u>2733.72</u>	<u>126.40</u>	<u>63.20</u>	Original
14	1594.21	253.02	126.51	32	2779.23	121.35	60.67	
15	1685.30	242.90	121.45	33	2822.93	116.49	58.25	
16	1772.74	233.18	116.59	34	2864.87	111.83	55.92	
17	1856.68	223.86	111.93	35	2905.14	107.36	53.68	Final
18	1937.27	214.90	107.45					

The first notable approximation concerns the determination of the length of the longest elements. A standard equation for determining this length (l_1) follows.

$$l_{1\pi} = \frac{492}{f_1}$$

The constant used to obtain the length in feet is simply the value that sets the length at a physical half-wavelength. Some calculating scheme set the length based on a frequency 2% to 3% lower. The practical goal is to arrive at an element length that will serve as the “reflector” substitute in this non-parasitic array. For any practical element diameter, a physical half-wavelength is already long relative to an electrical half-wavelength. We shall see why some

programs add further length as we explore various implementations of the dimensions in the table.

In fact, the self-resonant frequency of the longest element in the table varies according to the diameter that we assign to it. For diameters ranging from 0.1" (comparable to a wire element) up to 2" (not uncommon in LPDAs composed of aluminum tubing), the self-resonant frequency varies from 13.3 MHz down to 13.0 MHz, a 2.3% change with diameter changes.

However, the simplistic calculation of the longest element also fails to account for a fundamental factor that affects the performance of every array based on the use of an inter-element phase line. The proximity of the elements ensures that the elements receive energy from two sources: the energy supplied via the phase line and mutual coupling. Mutual coupling also alters the impedance at the element center relative to its value when treated as an isolated element. Therefore, depending upon the characteristic impedance of the phase line, the element diameters, and the selected values of τ and σ , we may find some versions of the array that operate satisfactorily nearly 15% below the lowest operating frequency and others that barely meet specifications at the lowest operating frequency.

It is possible to calculate a length-to-diameter (L/d) ratio for an array's element. The ratio will only be constant if the element diameters taper by the factor τ along with their lengths. (The current version of LPCAD builds this condition into the design that it presents.) However, many LPDAs use a constant or uniform diameter for all elements, especially those designed for VHF/UHF applications and those HF arrays composed of wire elements. As a consequence, the L/d ratio undergoes continuous change as we proceed from one element to the next. Even HF arrays making use of stepped-diameter element tubing schedules rarely end up with τ -tapered elements, but instead usually have a varying L/d ratio that falls somewhere between τ -tapered elements and uniform-diameter elements. (The need to design stepped-diameter tubing schedules to anticipated wind load specifications precludes the use of either uniform-diameter or τ -tapered values.)

Variations in the L/d ratio result in variations in the mutual coupling between adjacent elements in an LPDA. The actual L/d ratio finds direct application in the calculation of two important LPDA design parameters: the radiation resistance (or feedpoint impedance) and the characteristic impedance of the phase line. We may approximate the radiation resistance (R_0) from the following equation (although computer programs often set it as a user input):

$$R_0 = \frac{Z_0}{\sqrt{1 + \frac{Z_0}{4\sigma'Z_{AV}}}}$$

To find the value of the radiation resistance, we need to know 3 values: the phase-line impedance, the spacing factor, and the average characteristic impedance of any dipole in the array. Z_0 for the phase line emerges from the following equation.

$$Z_0 = \frac{R_0^2}{8\sigma'Z_{AV}} + R_0 \sqrt{\left(\frac{R_0}{8\sigma'Z_{AV}}\right)^2 + 1}$$

The equation also makes use of the spacing factor, which we can easily calculate:

$$\sigma' = \frac{\sigma}{\sqrt{\tau}}$$

Variations on these equations exist in some treatments of the design progression, but the common critical factor in all of them is Z_{AV} , the average dipole characteristic impedance.

A common equation for calculating Z_{AV} follows:

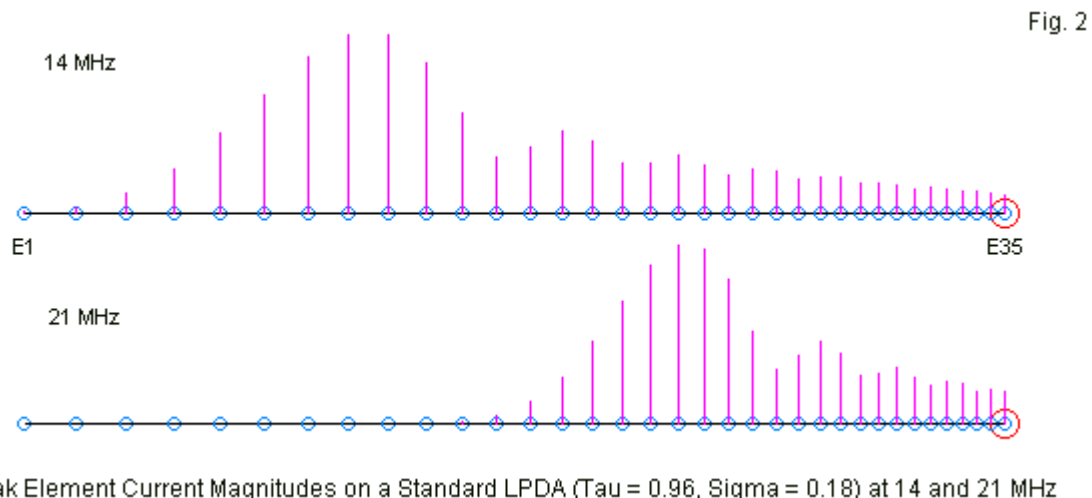
$$Z_{AV} = 120 \left[\ln \left(\frac{l_n}{diam_n} \right) - 2.25 \right]$$

The central ratio is simply the L/d ratio. However, we have a fixed ratio only if the element diameters follow the same tapering as the element lengths. For all other conditions, there is no single L/d ratio. (In fact, there are some LPDA designs that have employed a varying phase-line Z_0 , some all the way along a design and others for part of the distance from the feedpoint toward the rearmost element.) Theoretically, if we use uniform-diameter elements, we should re-calculate the phase-line Z_0 between each element pair. Where elements are very thin as a function of a wavelength, the change per step is small and the array will operate reasonably well with a constant value of Z_0 .

These notes do not void standard LPDA design procedures. Very good designs have emerged from their use, despite the fact that the electronic portions of the procedure use approximations. Indeed, good designs result even when we fail to appreciate the content of some steps and blithely ignore precisely what the equations tell us. Nevertheless, both the approximations in the progression and the further approximations that we use in formulating a design do have interesting consequences.

Low-End, High-End, and the “Active Region”

LPDA performance requires critical attention to 2 parts of the operating passband: the low end and the high end. The goal of every LPDA design is to achieve performance at both ends of the passband that equals to the degree possible the performance in the middle-frequency portion. We may begin our appreciation of current trends by looking at an array with very even low-end and middle-frequency performance, as shown by the peak current distribution along the length of the array in **Table 1** using all 35 elements. **Fig. 2** shows the distribution at 14 and at 21 MHz. The array employs a 255- Ω phase line to arrive at a target feedpoint impedance of about 200 Ω .



One important aspect of the curves is the fact that the 14-MHz version shows a complete cycle to the rear of the most active element, thus ensuring full performance at the lowest operating frequency. In fact, the virtually inert E1 element suggests that the array is longer than

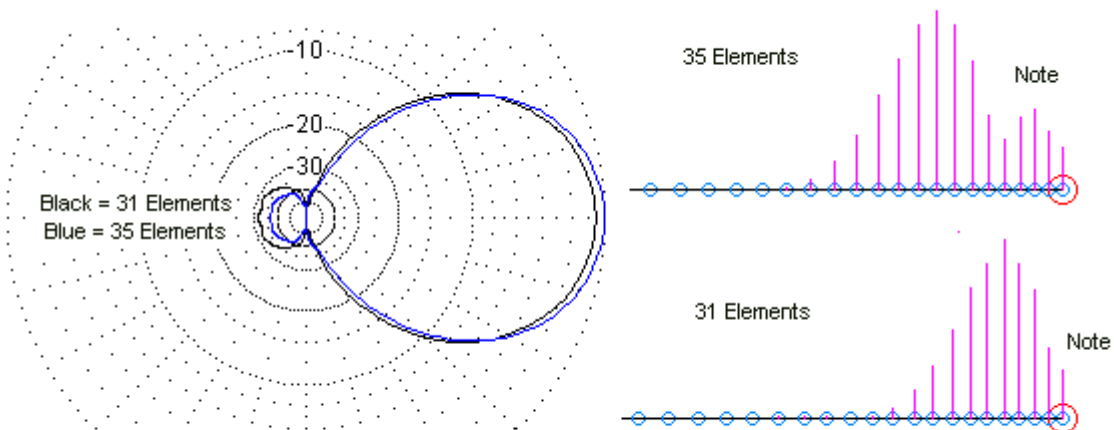
it needs to be. In fact, I specifically selected high- τ , optimum- σ arrays for this exercise to ensure that the rearward portions of the arrays remained inert at all operating frequencies. The subject of anomalous frequencies appears in detail in *LPDA Notes*.

The most important facet of the curves is that it demonstrates that every element forward of the most active element is significantly active. Moreover, the density of the element population is sufficient to show the cycles of peaks and valleys in the peak current value along the array. The second peak in the current for this sample array is 5 to 6 elements ahead of the most active element. (The 14-MHz curve shows two elements with approximately the same peak current, which prevents us from refining the position of the secondary peak any more precisely. However, the length of the element with the second current peak is a power of τ times the length of the element with the first peak.) A misunderstood idea related to LPDA designs is the notion of an “active region.” In the 1960s, numerous sources treated the elements very much like Yagi elements and restricted the range of activity to just a few elements on either side of the most active element. Even Kraus treats the forward portion of the active region in vague terms. (See endnote 2.) In fact, the active region extends from well behind (but finitely so) the most active element all the way to the feedpoint element and at least through the second current peak..

As we increase the operating frequency, we lose available room on the array for more than the most active element and a small number of elements on either side. For example, the subject array has both 31-element and 35-element versions, corresponding to design limits of about 47 and 52 MHz, respectively. The lower limit corresponds to the use of 1.3 times the highest operating frequency to arrive at the length of the shortest element. **Fig. 3** shows what happens under each of the two conditions.

Note: Elements 1 - 31 identical for both LPDAs.

Fig. 3

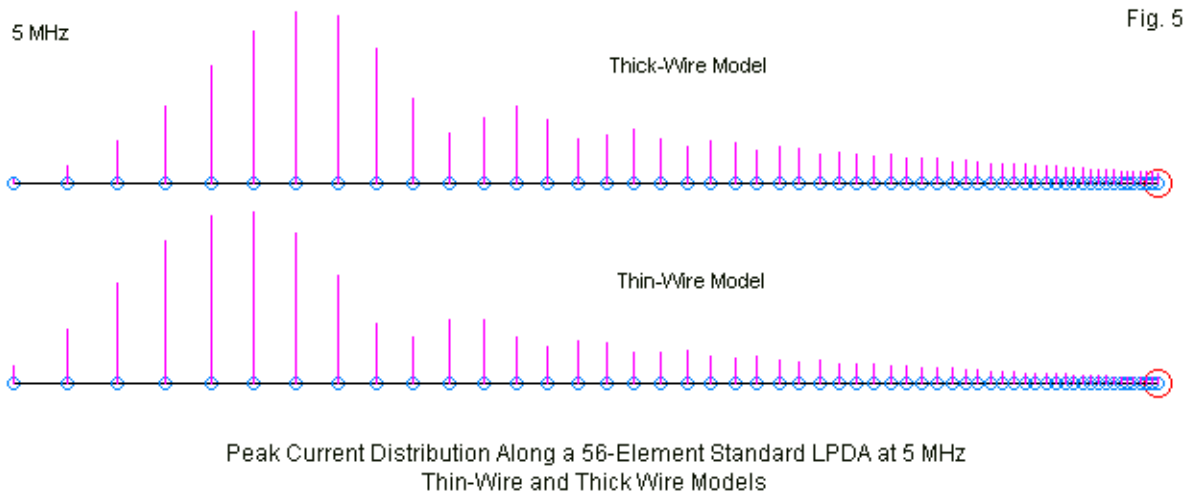
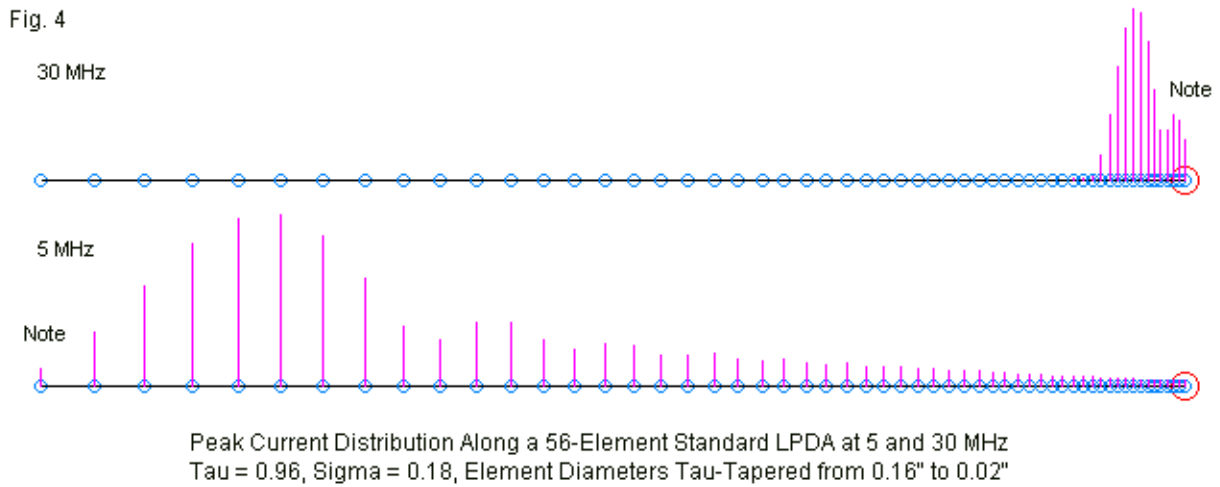


Peak Element Current Magnitudes on a Standard LPDA ($\tau = 0.96$, $\sigma = 0.18$) at 30 MHz with Overlaid Free-Space E-Plane Patterns Using 31 and 35 Elements

With the standard calculation and only 31 elements, the current distribution curve shows only a single peak. The result, as shown in the overlaid free-space E-plane patterns at the left, is a reduction in forward gain and increased rearward radiation. With 35 elements, we obtain a gain value much closer to the mid-band value, with an improved front-to-back ratio. Note that the current distribution curve for this version of the array includes two complete cycles, a condition we might think of as the minimum for smooth LPDA performance across the entire

passband. Indeed, it might be useful in LPDA design to drop the notion of the so-called active region and to replace it with the conditions required for proper top-end performance.
Bottom-End Position Variables

The initial examination of the 31- and 35-element 14-30-MHz LPDAs led me to review a design developed to use as a comparator with Extended Aperture LPDAs. The design consisted of 56 elements for service in the 5-30 MHz range. The total length of the array was about 775' using uniform 0.16"-diameter elements. **Fig. 4** shows the low-end and the top-end current distribution curves. We may note almost in passing that the 5-MHz graphic shows a complete cycle at the low end of the band, plus a number of secondary curves proceeding down the line of elements until the variations are too small for locating the peak-current element in each case. At the upper end of the band is a 30-MHz distribution curve that shows the requisite 2 cycles for good high-end performance.



The factor that called this model to my attention was the length of the shortest element: 120.9" long or self-resonant at about 47 MHz. In contrast, the shortest element of the 35-element 14-30-MHz array called for a front element that was 107.4" long or self-resonant at

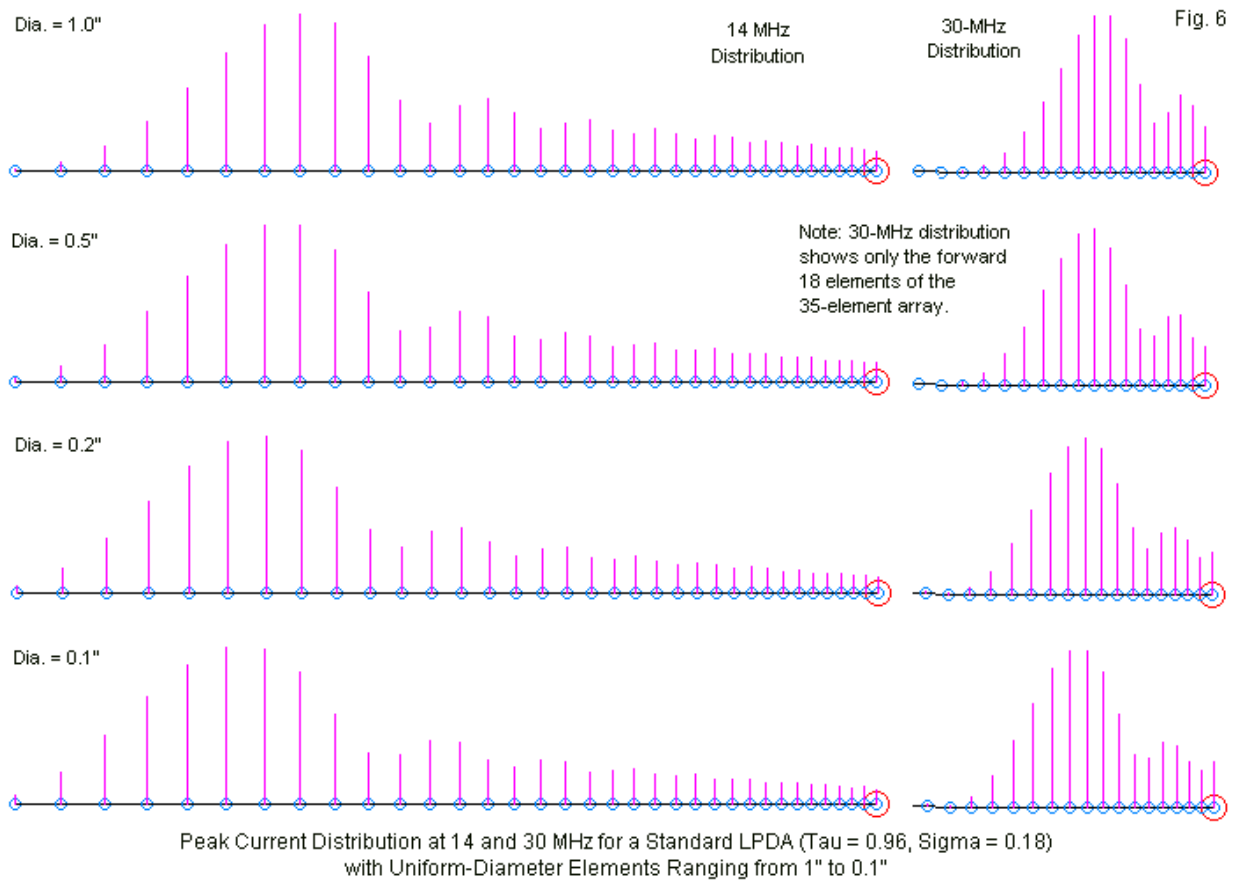
about 53 MHz. However, the elements on the array shown in **Fig. 2** and in **Fig. 3** are much thicker than 0.16". Therefore, I increased the element diameter to 2", a 12-fold increase.

Fig. 5 shows the results of the exercise. The "simple" act of increasing the element diameter displaced the low-end current distribution curve forward along the array relative to the original thin-wire model. The increase in element diameter has two effects. Perhaps the lesser of the two is the lowering of the individual element self-resonant frequencies. As earlier noted, changes of this order alter the self-resonant frequency by about 2% or so. More complex is the mutual coupling between adjacent elements, coupling that is naturally higher in the thick-element model. The combined result is a shifting of the position of the most active element by about 1.5 elements between the two extremes.

The results for the 56-element array suggested that perhaps a more systematic exploration might be useful.

Uniform-Diameter Element Models of the 35-Element 14-30-MHz Model

The first step was to provide the 35-element 14-30-MHz array with uniform-diameter elements of various sizes. The elements lengths, element spacing, and the 255-Ω phase line did not change as the element diameter decrease from 1.0" down to 0.1", a 10:1 range. **Fig. 6** shows the outcome in terms of current distribution at both 14 and 30 MHz.



The decreasing element diameter shows a continuous progression rearward for the most active element at both ends of the operating spectrum. I terminated the element diameter range at values that resulted in no significant decrease in performance at either end of the spectrum, as shown by the data in **Table 2**. The data use 14, 21, 28, and 30 MHz as check frequencies, largely because the first three frequencies represent the low end of amateur bands.

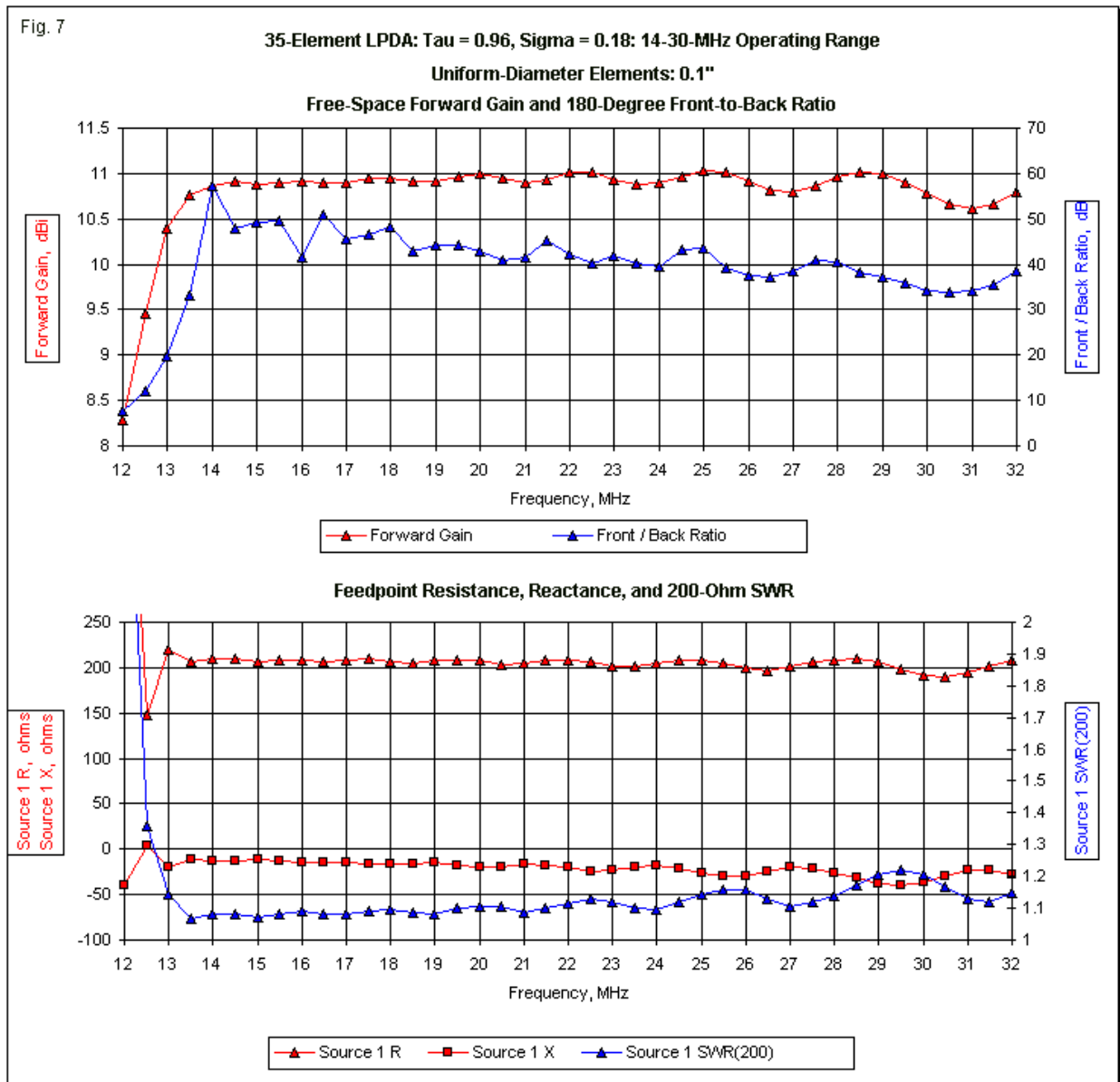
Table 2. Spot free-space performance data for the models used in Fig. 6. All models have the same 35 elements (see Table 1) and use a phase-line Z_0 of 255 Ω .

Element Dia. In.	Frequency MHz	Max. Gain dBi	F-B Ratio dB	Impedance R +/- jX Ω	200- Ω SWR
1.0"	14	11.56	47.22	186 – j17	1.12
	21	11.68	40.52	187 – j29	1.18
	28	11.30	32.36	166 – j43	1.35
	30	11.42	38.14	190 – j36	1.21
0.5"	14	11.37	47.10	196 – j16	1.09
	21	11.45	43.15	196 – j22	1.12
	28	11.37	35.18	190 – j45	1.27
	30	11.03	34.09	187 – j24	1.15
0.2"	14	11.09	48.86	204 – j13	1.07
	21	11.10	42.82	202 – j18	1.09
	28	11.21	39.04	205 – j32	1.17
	30	10.84	33.31	184 – j30	1.20
0.1"	14	10.87	57.28	210 – j13	1.08
	21	10.90	41.52	205 – j16	1.09
	28	10.96	40.39	209 – j26	1.14
	30	10.78	34.33	192 – j36	1.21

In very broad terms, we can readily see that as we decrease the element diameter, the average gain decreases. As well, we find an increase in the 180° front-to-back ratio. These parameters are almost, but not quite, independent of the feedpoint impedance changes. In fact, to provide the thick-element models with feedpoint impedance values closer to the target impedance, we would need to change the Z_0 of the phasing line to a higher value. In turn, this maneuver would create slight changes in the spot values for gain and front-to-back ratio.

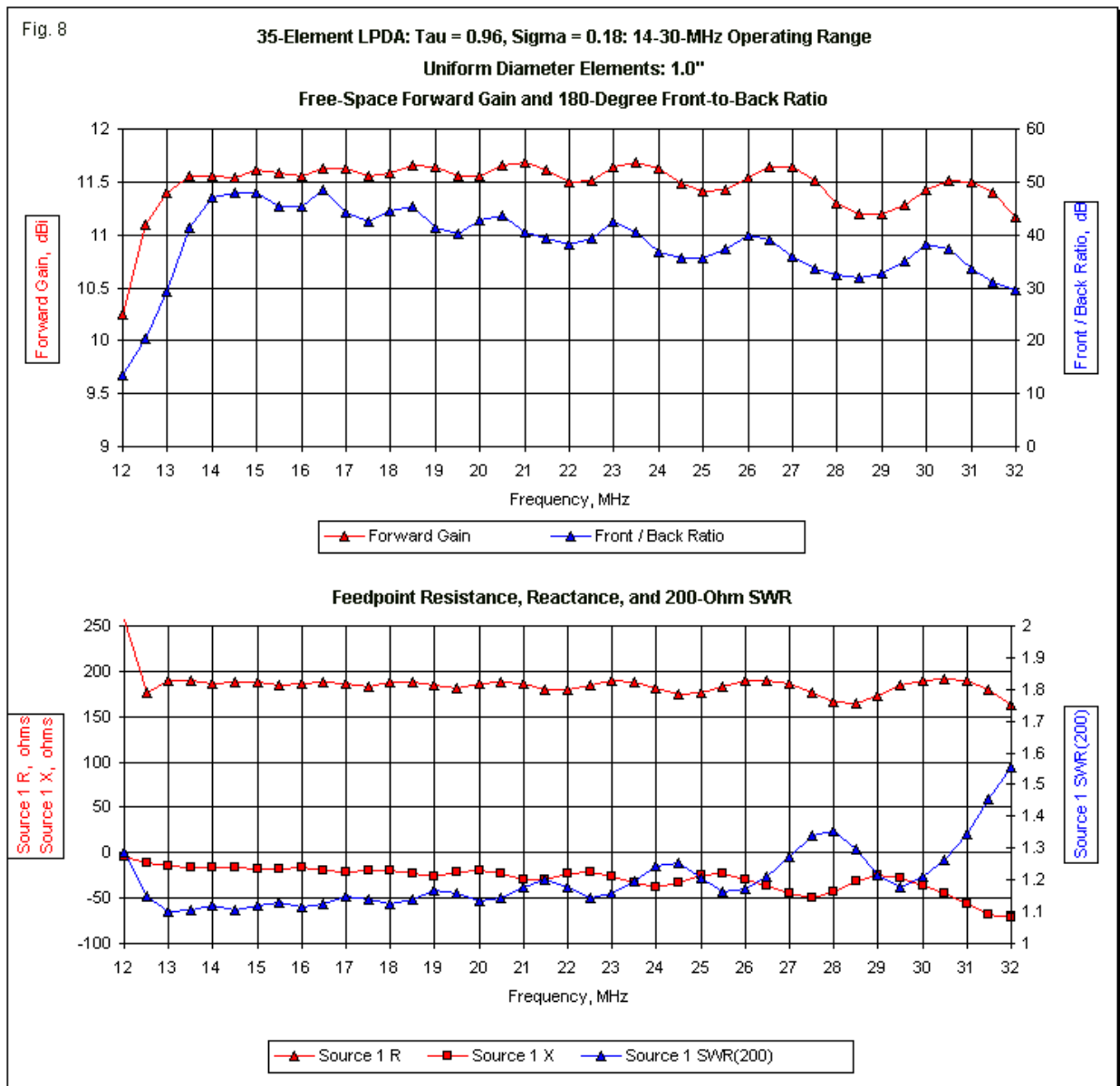
Perhaps the most significant change following small changes in the line Z_0 is the position of the peaks and valleys in the curves for the various parameters that define LPDA performance over a broad range. Every LPDA performance curve, when swept over the operating span and beyond, shows undulations in the exact performance level. **Fig. 7** provides curves the 0.1" element version, while **Fig. 8** shows the performance with 1.0" diameter elements. I carried out the sweep from 12 to 32 MHz to gauge the potential performance above and below the specified operating range of each array. The sweep increment is 0.5 MHz, a value that gives the low-end performance less smooth curves than we find toward the upper end of the spectrum. The resistance and reactance ranges (Y-axis) have limits of –100 Ω and +250 Ω to allow for easier comparison of values between graphs, even though the values at frequencies below 14 MHz may rise off scale.

Fig. 7 shows gain and front-to-back values that undulate, as predicted. As well, they do not reach maximum and minimum values at the same frequency. Moreover, the gain and front-to-back peaks do not coincide directly with the feedpoint resistance and reactance values. As we make small changes in the operating frequency, the element impedances change, resulting in small variations in the energy supplied to each element. Combined with the mutual coupling between adjacent elements, the consequence is a constantly shifting balance among the parameters.



As one might expect from the current distribution curve in **Fig. 6** for the 0.1" elements, the thin-wire model reaches full gain and front-to-back potential at or just below the beginning of the operating passband. The gain and front-to-back curves between 28 and 30 MHz are interesting, since they both show a downward slope, but with a reversal toward more positive values at 32 MHz. **Fig. 8**, for the 1.0"-element version of the array, shows opposite sloping in the 28-30-MHz area. In addition, the overall curve of the array with thicker elements shows a

greater downward trend as we reach the upper portions of the operating range. In general, the 1" elements are too large for the selected phase-line Z_0 at the higher end of the spectrum. The spot impedance values reflect this condition.



In Fig. 6, we saw the fat-element curve displaced forward, with nearly inert elements at the array rear end. These elements are eligible for LPDA duty at frequencies below the operating range. As the sweep in Fig. 8 shows, the thick-element version of the array is capable of very reasonable performance down to nearly 13 MHz. Even the impedance values are quite good to some frequency below 13 MHz. At the top end of the spectrum, the array with 1" elements shows a rapid increase in the 200- Ω SWR line, due both to an average decline in the feedpoint resistance and a rapid trend toward increased capacitive reactance with increasing frequency.

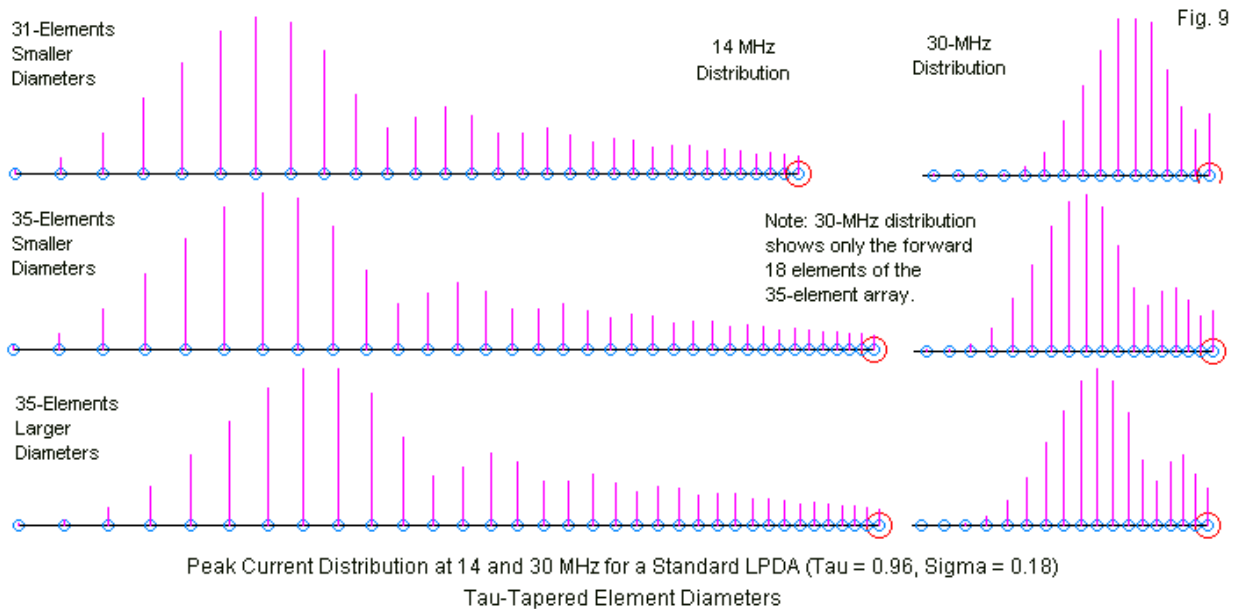
Although many LPDA design use a single diameter for all elements, the practice departs from basic LPDA theory, which presumes that element diameters have a relatively constant L/d

ratio. The departure is certainly not fatal, since any of the sample LPDAs with a 2:1 frequency range (or scaled versions of them) would likely perform quite adequately for most applications. The 2900" (242') boom length may be prohibitive for HF use as a horizontal beam, but the array would be useful in the UHF range and above.

τ -Tapered Elements and a Constant L/d Ratio

I remodeled the 31- and 35-element 14-30-MHz LPDAs to use τ -tapered elements that produced constant values for the L/d ratio. The smaller element sizes show a ratio of 860:1, while the larger elements show an L/d value of 215:1. The small rear element diameter is 0.5"; the larger counterpart is 2" in diameter. All other factors remain the same, including the element lengths, the element spacing, and the 255- Ω phase line.

Fig. 9 supplies the relevant current distribution curves for both 14 and 30 MHz. The short array and its small-element 35-element mate show virtually the same current distribution at 14 MHz—allowing for the fact that graphic limitations prevented a perfect alignment of every element. At 30 MHz, the top pair of curves shows the consequences—even with τ -tapered elements—of having an inadequate number of forward elements. The 31-element array has just the start of the second current cycle at the forward-most element. In contrast, the 35-element array with smaller diameter elements shows two complete cycles.



The lower curves are both for 35-element arrays, but with a 4:1 difference in each element diameter. The larger-diameter version shows the forward displacement of both sets of curves. At both frequencies, the displacement of the most active elements is just about one full element along the array. Nevertheless, the larger-diameter array has enough elements to allow the virtual completion of the second current cycle at 30 MHz. Therefore, we should expect a relatively smooth gain curve across the operating spectrum.

We shall follow the same procedure that we used with the uniform-diameter models. First, we shall sample the data at 14, 21, 28, and 30 MHz for all three arrays. **Table 3** gives the data

in the same format that we used for **Table 2**. Following the data set, we shall examine 12-32-MHz sweeps of all three arrays for additional information on their performance characteristics.

Table 3. Spot free-space performance data for the models used in Fig. 9. All models use elements in Table 1 and have a phase-line Z_0 of 255 Ω .

Array Version	Frequency MHz	Max. Gain dBi	F-B Ratio dB	Impedance R +/- jX Ω	200- Ω SWR
31 El. Small	14	11.11	45.56	205 - j13	1.08
Elements	21	11.16	40.86	206 - j27	1.14
L/d = 860	28	10.99	34.64	208 - j47	1.26
	30	10.30	29.40	169 - j29	1.31
35 El. Small	14	11.18	48.69	208 - j12	1.07
Elements	21	11.08	43.85	206 - j17	1.09
L/d = 860	28	11.10	40.14	209 - j29	1.16
	30	10.76	34.04	188 - j31	1.19
35 El. Large	14	11.50	48.94	195 - j14	1.08
Elements	21	11.51	42.78	196 - j25	1.14
L/d = 215	28	11.25	34.55	184 - j45	1.28
	30	11.05	35.92	192 - j25	1.15

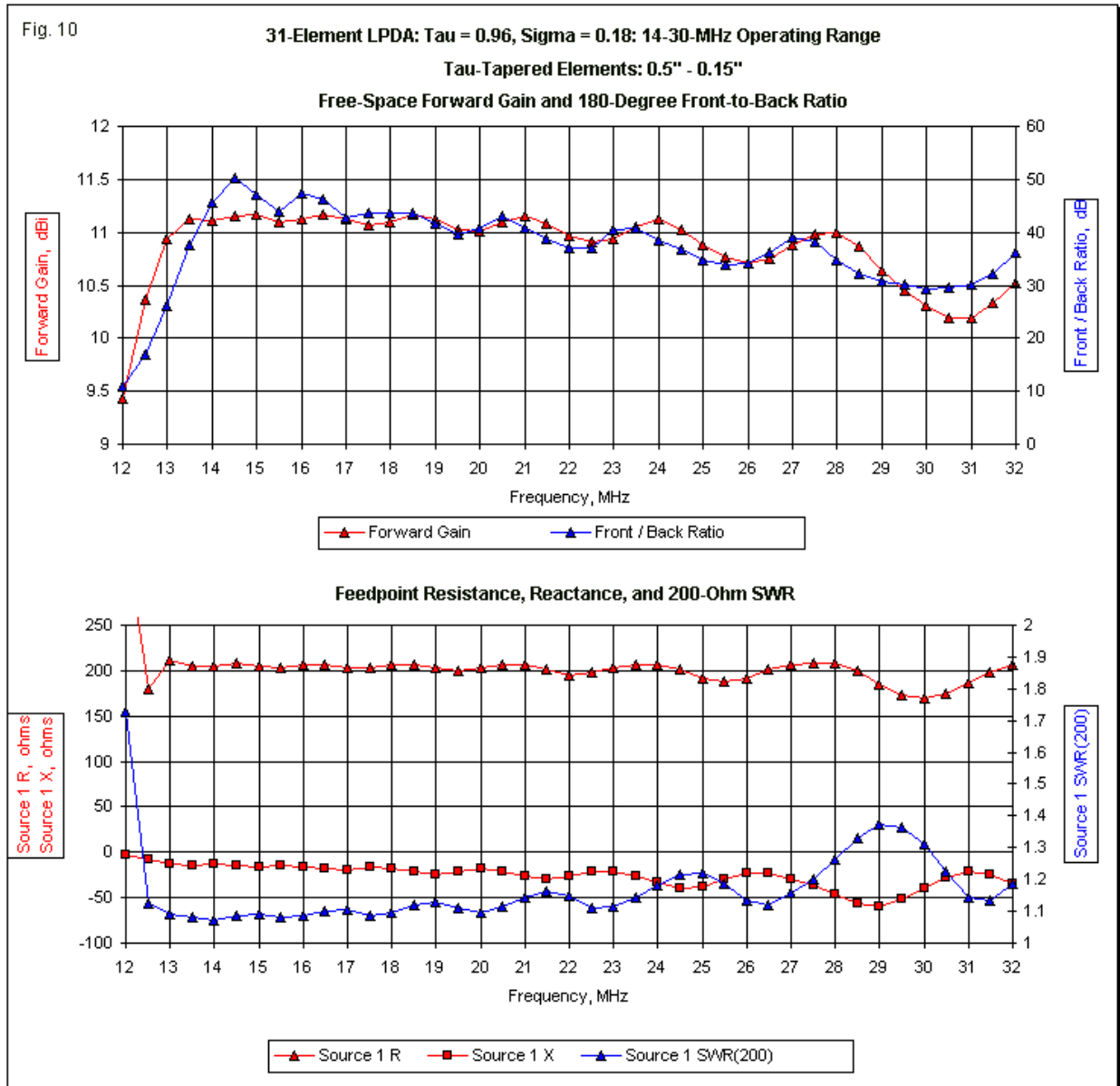
Between the shorter and longer small-element arrays, the general trends show improved performance at 28 and 30 MHz when we add the final 4 elements. We not only find better gain and front-to-back ratio values, but also smaller excursions in the feedpoint impedance and the 200- Ω SWR. Between the 35-element versions with different element diameters, we encounter the rise in gain that is due to the use of generally thicker elements. We cannot from the spot checks assign a particular average value to the gain rise, since the frequencies do not necessarily appear at coincident places on the sweep undulations. As well, the phase-line Z_0 is not optimal for the larger diameter element set. (The design equations suggest a value of 284 Ω .)

The combined or averaged values for 28 and 30 MHz do not show any negative effects from the forward displacement of the current curves in the large-element set. All that we appear to see are the results of increasing the total set of element diameters to arrive at a small L/d ratio. To examine the situation more closely, we must again turn to frequency sweeps of the array at 0.5-MHz intervals from 12 to 32 MHz. As in the first set of sweeps, I have limited the Y-axis range for the resistance and reactance to permit more ready comparisons among the sweep graphs. In addition, for this set of frequency sweeps, I have set the free-space gain range on the Y-axis to limits of 9 and 12 dBi.

Fig. 10 supplies the sweeps for the 31-element array using the smaller set of element diameters. The gain and front-to-back curves show a minimum useful frequency of no lower than about 13.5 MHz. Like most LPDAs of significant proportions (that is, with a high value for τ and an optimized value for σ), the usable SWR range extends below the minimum performance range.

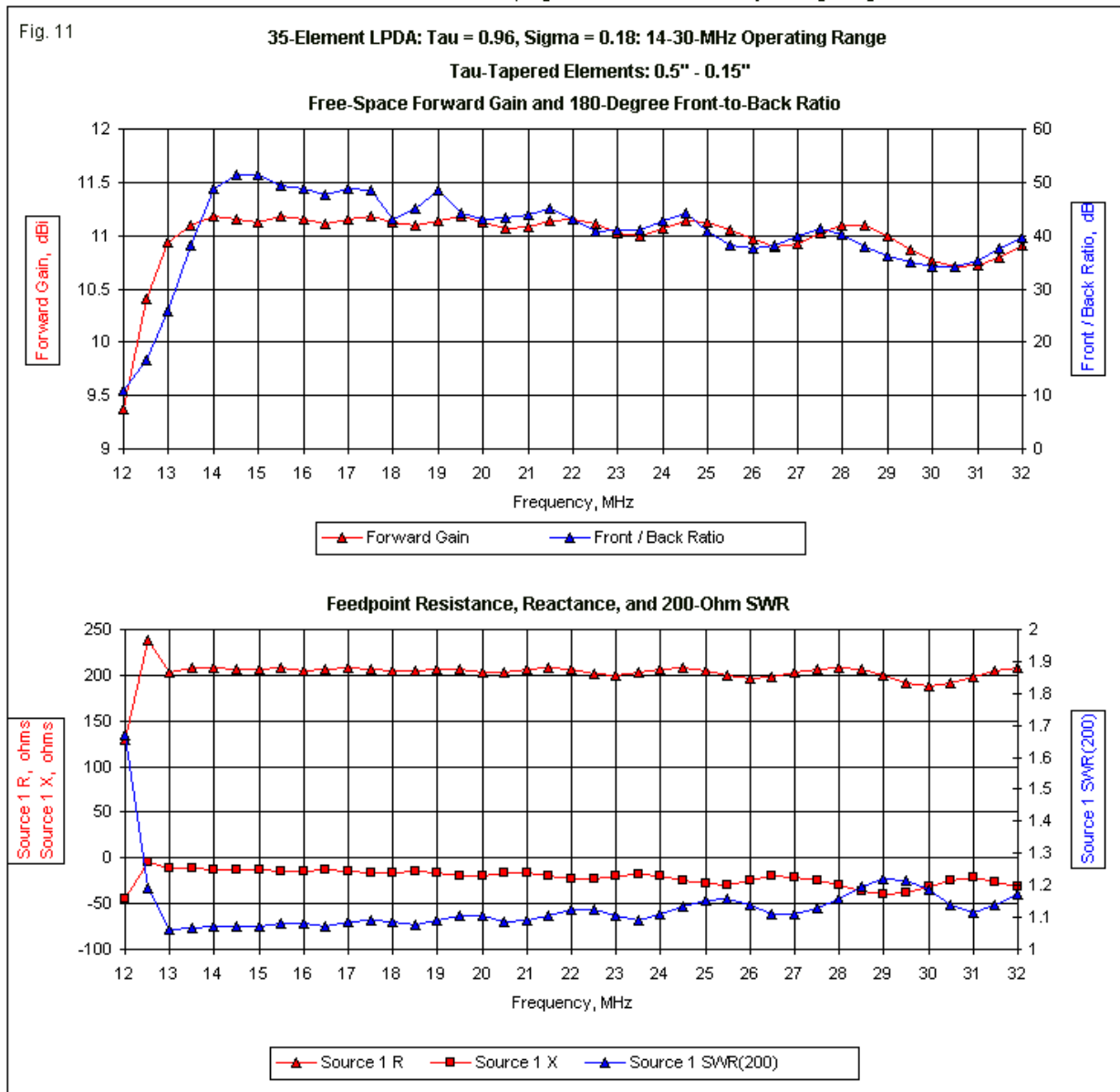
As we move upward in frequency, the curves show a significant downward trend in both the free-space gain and the 180° front-to-back ratio. The beginning of the trend occurs at a lower

frequency than we might have expected from the spot check, because 21 MHz values are nearly at the peak of the undulations. The average value in this region is already below the average value for lower frequencies. In addition to the declining gain and front-to-back values, we also see the effects of using too few forward elements in the SWR curve. Although the average value may be acceptable, we discover rapidly rising peak values, most notably around 29 MHz. The SWR trends result not only from the fluctuating values of resistance and reactance, but as well to the significant increase in the average capacitive reactance.



Many of the difficulties that we encounter in the 31-element sweep find amelioration in the 35-element array that uses the same L/d ratio. **Fig. 11** shows the differences that the added 4 elements make to performance across the operating pass band. Since the elements for the lower frequencies are essentially the same, the lowest frequency that shows minimally acceptable performance values remains at about 13.5 MHz. Unlike the low-end impedances values for the 31-element array, the values that apply to the 35-element LPDA all fall within the

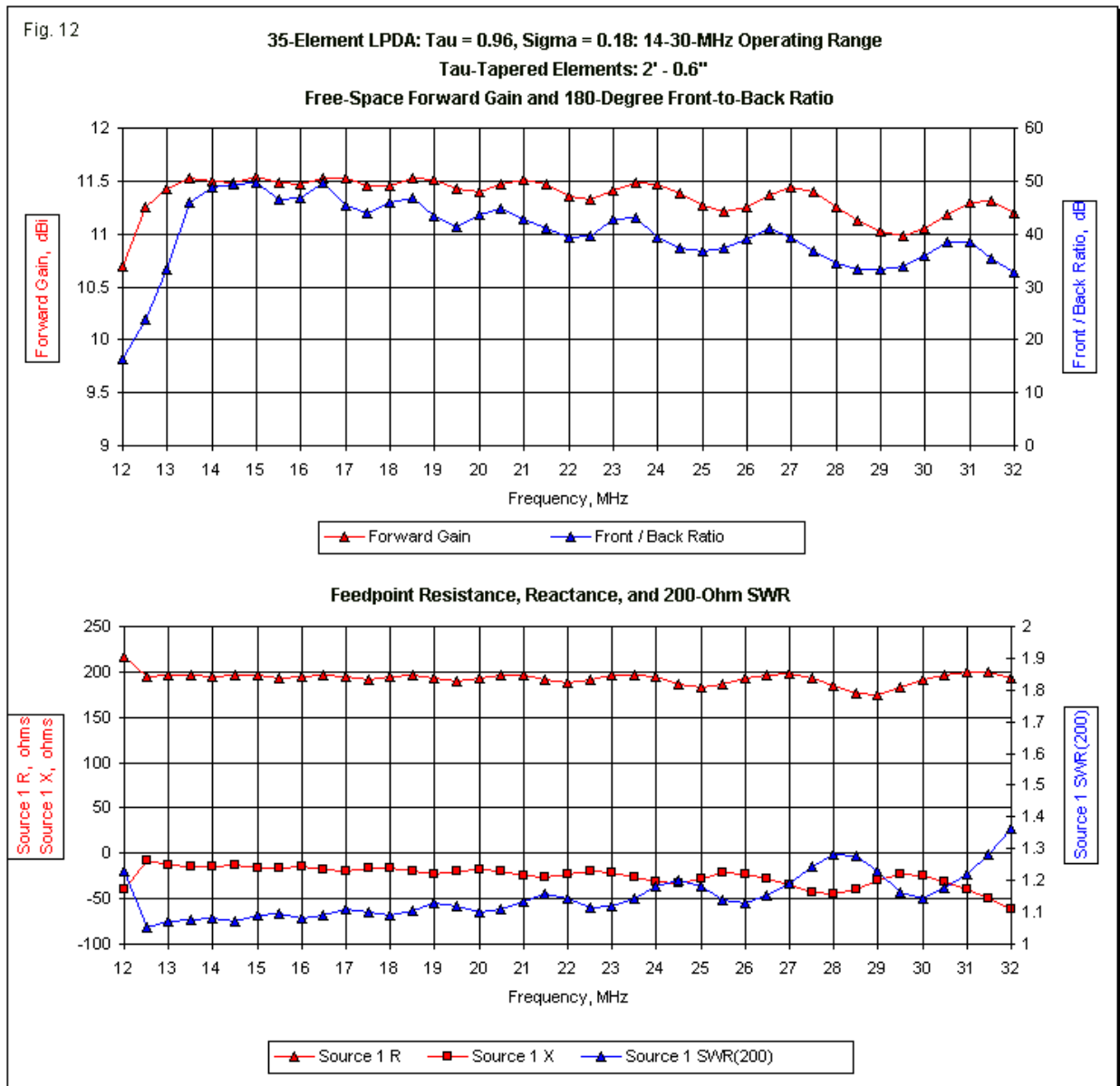
graphing limits. Although a general downward trend in gain and front-to-back values is apparent in the longer array, it is not as extreme as in the shorter version. Also significant is the improved smoothness of the SWR curves. Although it undulates, the peaks within the passband are not nearly as great at the upper end of the operating range as in the graph for the shorter LPDA. The source lies in a combination of resistance and reactance values that fall within narrower limits.



The forward displacement that we found all along the current distribution curves for the 35-element LPDA with larger elements results in a minimum useful frequency about 0.5 MHz lower than for the comparable array with smaller elements. **Fig. 12** not only shows improved gain and front-to-back ratio values below 14 MHz, but as well, the SWR limits fall below 12 MHz.

As we increase the operating frequency, we find some interesting differences between the two 35-element arrays. The free-space gain of the array with fatter elements tends to hold up

better than the gain with thinner elements. However, the front-to-back ratio tends to fall off more quickly as we increase the elements diameters (or decrease the L/d ratio). To what degree the differences result from the increase mutual coupling among thicker elements and to what degree the differences result from the slightly low phase-line Z_0 has not been explored. The increased peaks in the SWR values at higher frequencies in the LPDA with larger elements suggest that the phase-line Z_0 may play some role, although perhaps not a total role. Note that the upper-end peaks in SWR are significantly lower than with the uniform 1" diameter model, as shown in the sweep curve in Fig. 8.



If you examine all of the sweep graphs presented so far, several features should become relatively apparent. First, in all of the LPDA versions, the front-to-back ratio reaches a peak value at a lower frequency than the forward gain. As well, the resistance and the reactance peak fail to line up with either the gain or the front-to-back value. These features of LPDA

sweeps show the complexity of the relationships among the elements and the feeding and phasing system used.

More significant to these notes is the role of element size and taper in the positions of the current distribution curves. Whether the elements are uniform in diameter or τ -tapered, larger elements and the resulting increase in mutual coupling among adjacent elements tends to displace the peak current at any operating frequency more forward in the array. The consequences may be as equally important for either end of the operating spectrum. Fatter elements may require more additional short elements to achieve acceptable performance levels at the upper limits of the operating spectrum.

Changing the Feedpoint Impedance Target and the Phase-Line Z_0

Suppose that we wish a target feedpoint impedance closer to the value of the ubiquitous 50- Ω coaxial cable. We can design the 35-element LPDA to that goal without changing the length or spacing of the elements. If we plug the goal into the sequence of design equations, we obtain in LPCAD a phase-line Z_0 of 75 Ω , the lowest value that it will allow. As a result of this limit, the feedpoint impedance comes out in the 60- Ω range, suitable for use with either 50- Ω or 75- Ω cable. The modified array uses the larger element set, with the diameter of the longest element set at 2".

If we compare the current distribution curve to the one for the 200- Ω large-element version of the array, we obtain the interesting result shown in **Fig. 13**. The use of a lower phase-line characteristic impedance changes the position of the current magnitude peaks at all frequencies. The new position is rearward by 2 full elements. At 14 MHz, we just include the full prime cycle. At 30 MHz, we find almost 3 cycles.

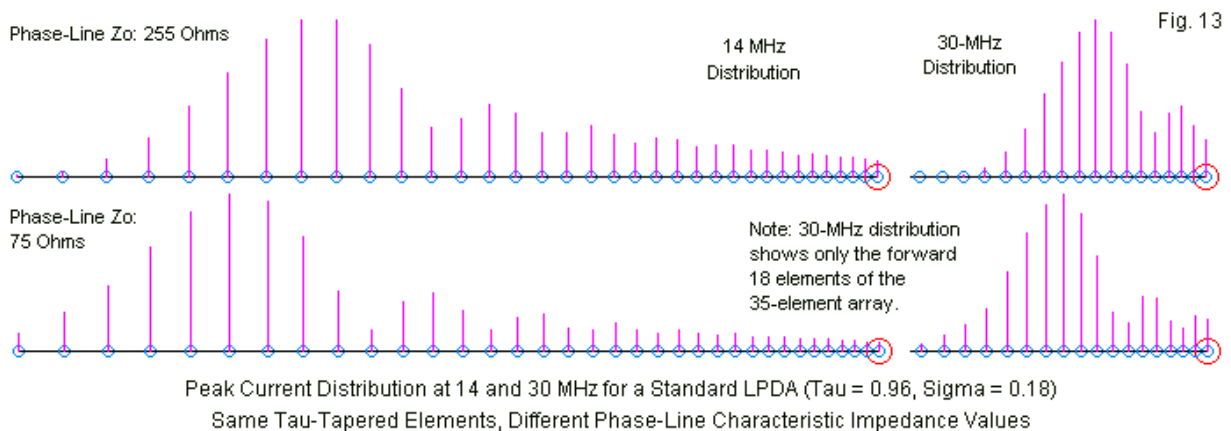


Table 4 provides sample performance data in parallel with the information in other tables. We may note from the outset that the lower impedance phase-line yields about 0.5-dB additional gain over the corresponding 200- Ω version of the same element set with no other changes. The appearance seems stable, but the front-to-back ratio appears to fluctuate.

Table 4. Spot free-space performance data for the new models used in Fig. 13. The model uses elements in Table 1 and has a phase-line Z_0 of 75 Ω .

Array Version	Frequency MHz	Max. Gain dBi	F-B Ratio dB	Impedance R +/- jX Ω	50/75- Ω SWR
35 El.	14	12.22	36.60	68 - j2	1.37/1.10
Large	21	12.50	23.89	69 - j3	1.38/1.10
Elements	28	11.91	46.61	66 - j3	1.32/1.15
L/d = 215	30	12.04	37.51	70 - j6	1.42/1.11

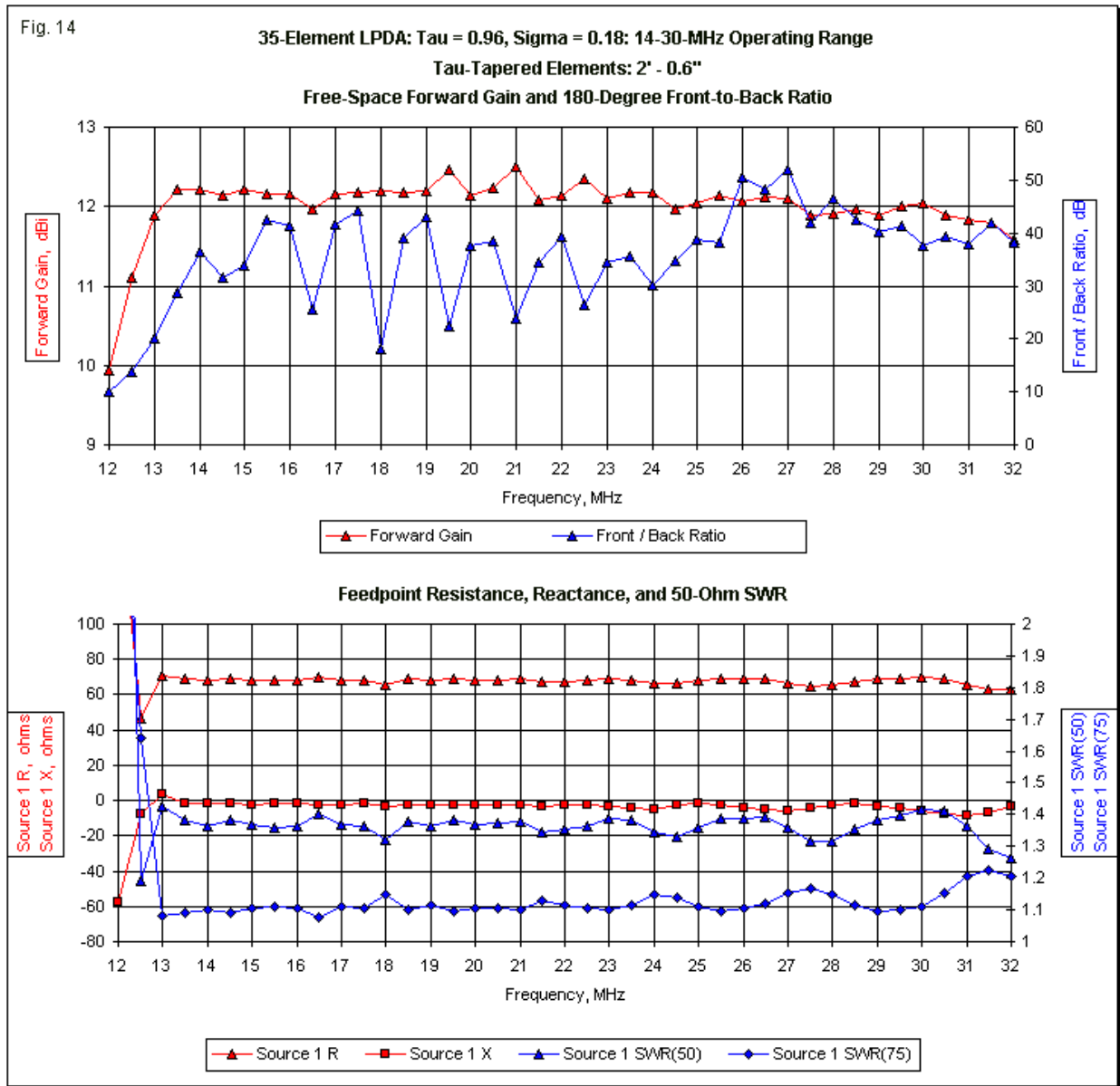


Fig. 14 supplies the sweep graphs on the revised array. Although the forward gain appears stable, the curve has a few small but sharp spikes. Some of the spikes correspond to equally sharp dips in the front-to-back ratio. At 18 MHz, the front-to-back ratio drops below 20 dB.

The usable range of performance and feedpoint values begins at about 13 MHz and extends beyond the upper limit of the graph. Within the usable range, the resistance, reactance, and the SWR values (referenced to both 50 Ω and 75 Ω) are all stable. Although the sweep indicates no anomalous frequencies, it may be wise to perform a set of sweeps over any span where a front-to-back value depression occurs, using very small increments between pattern samplings. Many sources recommend the use of phase-lines no lower than 150 Ω , due to the increased tendency of lower Z_0 values to yield anomalous frequencies that show either very reduced performance or even reversed patterns. As well, the anomaly may not show itself in the impedance category at precisely the same frequency as the maximum pattern disruption. These potentials are the price for the added gain produced from low-impedance phase lines.

Conclusion

These notes have tried to demonstrate the effects of element size on the placement of current maximums and minimums along a standard design LPDA. For a given set of values for τ and σ , the distance between the first and second current maximums is the same when measured in terms of the number of intervening elements. By judiciously setting the operating frequency of the 56-element array (4.85 MHz) and the 35-element array (13.2 MHz), I was able to obtain peaks on elements 5, 11, 15, 18, 21, 24, 27, 30, 32, and 35, counting from the rear. This exercise is limited by the fact that each element counts as an integer. The probable distance between the first and second peaks is closer to 5.75-6.0 elements or at intervals based on τ . This "element" distance between first and second current maximums holds true for every operating frequency within the design span for the array, as do the slowly shrinking intervals between lesser current maximums. Basic log-periodic theory calls for these peaks, although in sparsely populated LPDA designs, they do not show as vividly as in high- τ models.

We examined the use of both uniform-diameter and constant-L/d-ratio elements sets, and in both cases found that the larger the element diameter, the further forward in the array that current maximums appeared. One consequence of this phenomenon is often the need for greater numbers of short elements to allow the array to produce relatively even performance across the entire operating range specified for the design. In many cases, the self-resonant frequency of the shorted element must exceed 1.6 to 1.8 times the highest operating frequency.

We also explored briefly the consequences of changing the phase-line characteristic impedance, comparing a moderate value (255 Ω) to a low value (75 Ω). The lower value phase-line displaced the current peaks rearward. Indeed, a combination of a low-impedance phase line and very thin wire elements might force the addition of a new low-frequency element. More likely, in such cases, one should simply design the array by assuming a lowest design frequency below the actual lowest operating frequency.

The differing characteristics of the current distributions as we change element diameters and phase-line values can affect LPDA design. Element diameter changes alter the impedances of the individual elements and the mutual coupling between adjacent elements. Changes in the Z_0 of the phase line affect the energy directly fed to each element. These aspects of LPDA operation do not appear in the normal progression of LPDA design equations. If LPDAs remain interesting to various communications applications, we may one day see a computer program that takes these factors into account. Until that day arrives, detail exploration

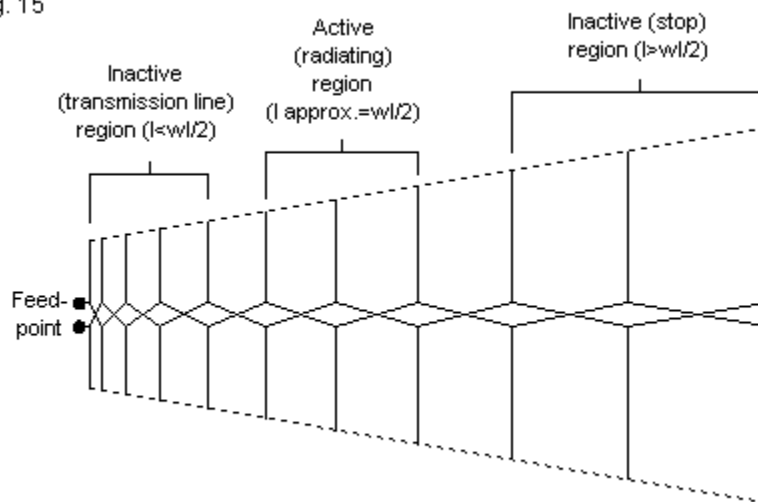
of a given design via NEC or similar modeling programs may be the analysis tools of choice— followed, of course, by manually implemented correctives.

End Notes

1. Examples of additional design procedures appear in Lo and Lee, *Antenna Handbook* (1993), Vol. 2, pp. 9-28, and in Balanis, *Antenna Theory: Analysis and Design*, 2nd Ed. (1997), pp. 561-563. Within amateur radio literature, see Rhodes' QST article of November, 1973 ("The Log-Periodic Dipole Array," pp. 16-22). An additional version of the design procedure appeared in "Log-Periodic Antenna Design," *Ham Radio*, December, 1979, pp. 34-39.

2. Kraus, in *Antennas*, 2nd Ed. (1988), p. 704 (Fig. 15-10), shows the active areas of an LPDA (following Isbell) in the terms listed in **Fig. 15**.

Fig. 15



Kraus Designations for LPDA Regions from Antennas (1988)

By the late 1990s, the understanding of element current levels had changed. For instance, see Stutzman and Thiele, *Antenna Theory and Design*, 2nd Ed. (1998), p. 268 (Fig. 6-40), show the peak current distribution along a 4:1 frequency-ratio LPDA at low, middle, and high frequencies within the operating range. The 18-element array clearly shows current activity at the lowest sampled frequency extending all the way to the most forward elements. Unfortunately, the sample array has too few elements to show clearly the cyclical nature of the current peaks or the correlation of the distance (as measured in the number of intervening elements) between the highest and the second highest peak regardless of operating frequency.